A simplified correlation between vertebrate evolution and Paleozoic geomagnetism

Corresponding Author: John P. Staub Unaffiliated researcher Email address: paleopjs@yahoo.com

Introduction

Geomagnetic polarity reversals occur randomly about two or three times per million years (Gradstein, 2012). The transition between the collapse of the Earth's protective magnetic shield and its subsequent regeneration can last thousands of years, and the effects on biota during this interim are unknown.

In 1963, Uffen raised the possibility that polarity reversals might increase extinction rates due to harmful solar and cosmic radiation. Others pointed out the Earth's atmosphere is our primary shield. Secular variations of a weakening geomagnetic field intensity show enhanced cosmic-ray production of ^{10}Be, ^{36}Cl, and ^{14}C in the stratosphere (McHargue, 2000). Reinforcing this view, age-dated Greenland ice cores contain relatively high concentrations of these isotopes aligned with polarity excursions (Raisbeck, 2006). DNA, despite active repair mechanisms, can be susceptible to ^{14}C decay (Sassi, 2014), and recently, Van Huizen (2019) showed weak magnetic fields can directly alter regeneration of worms. Volcanism (Courtillow, 2007), climate alteration (Harrison, 1974), low-frequency electromagnetic fields (Liboff, 2013), depletion of ozone (Huang, 2017), and the stripping of atmospheric oxygen (Wei, 2014) have been proposed as possible culprits, but Glassmeier and Vogt in their review of *Magnetic Polarity Transitions and Biospheric effects*, after listing numerous causations, found no evidence of effects (Glassmeier, 2010).

Sepkoski's 2002 marine fossil compendium shows minimal alignment of biota and polarity reversals—with one exception, family-level Paleozoic vertebrates.

In a previous study (Staub 2018), we showed a strong connection between geomagnetic activity and the initial twenty-million-year evolution of 27 separate clades. In this study, for simplicity and reproducibility, only eight major phylogenetic groups will be correlated with geomagnetism. And instead of an arbitrary twenty-million-year limit, we will concentrate on the competitive replacement model, where the early radiation of a clade's evolution ends at, or soon after, the intervention of a subsequent phylogenetic group.

PeerJ Preprints | https://doi.org/10.7287/peerj.preprints.28002v3 | CC BY 4.0 Open Access | rec: 31 Dec 2019, publ: 31 Dec 2019

Figure 1 Polarity Reversals and Distribution of Paleozoic vertebrates.

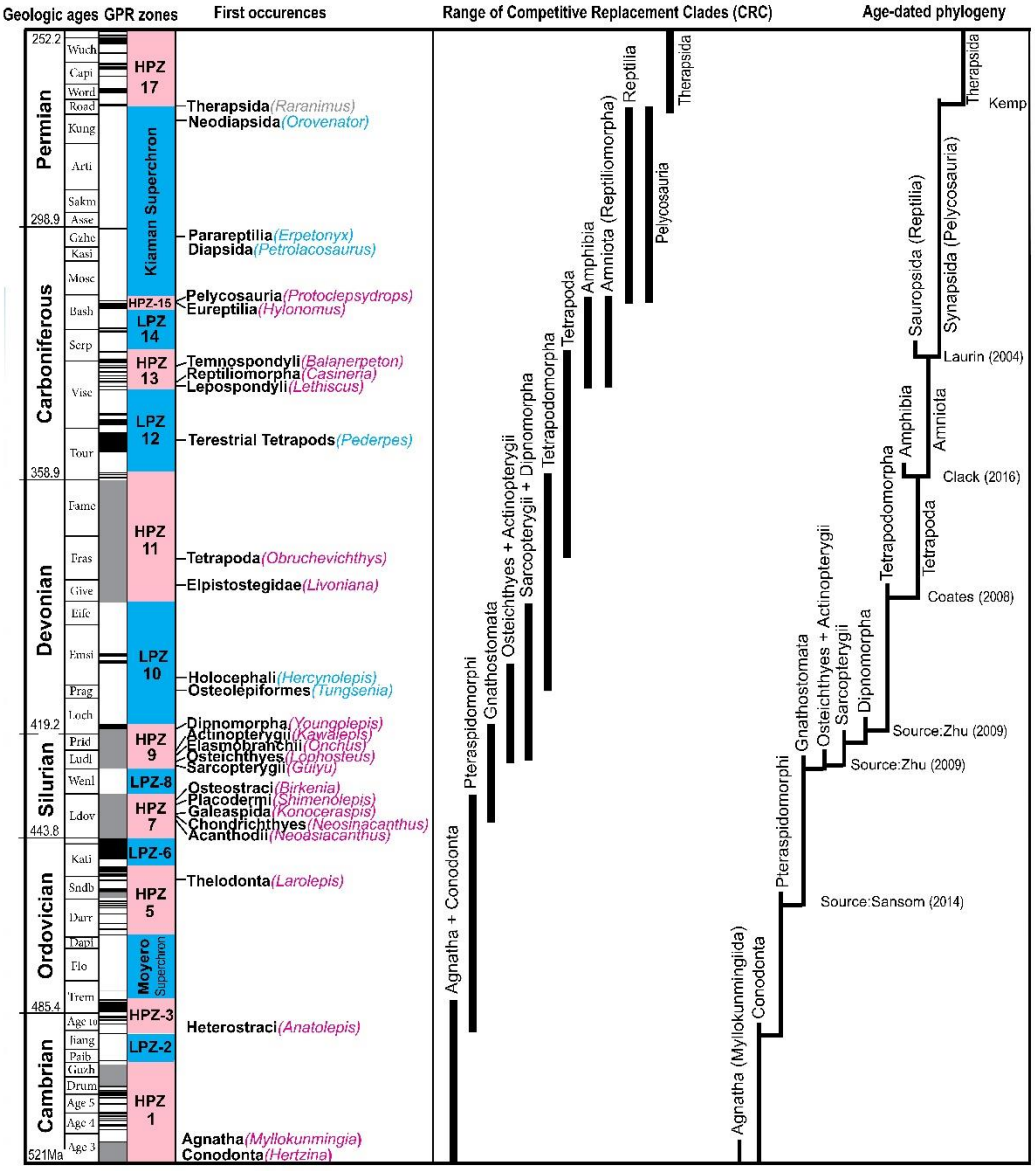

Figure 1: Columns (1) and (2): geologic periods and stages (Gradstein 2012). Column (3): geomagnetic polarity reversals from multiple sources (black is normal polarity; white is reversed; gray represents multiple reversals). Column (4): high (red) and low polarity (blue) zones. Column (5): FAD of originating genus of 28 clades. Column (6) shows the "early-phase" ranges of 11 major groups of Paleozoic vertebrates. Column (7): Possible age-dated phylogeny of Paleozoic vertebrates, with sources. For this study Sarcopterygii, Dipnomorpha, and Tetrapodomorpha are combined into a single group; in addition, the basal tetrapods, early amphibians and Reptiliomorpha are also combined.

PeerJ Preprints | https://doi.org/10.7287/peerj.preprints.28002v3 | CC BY 4.0 Open Access | rec: 31 Dec 2019, publ: 31 Dec 2019

Methods

Our compilation of 2104 Paleozoic vertebrate genera was generated from four sources: the Paleobiology database (paleobiodb.org); Benton's list of terrestrial vertebrates from the supplemental in *The first half of tetrapod evolution* (Benton, 2013); Sepkoski's 2002 marine compendium (Sepkoski, 2002); Zhao and Zhu's *Siluro-Devonian vertebrate biostratigraphy and biogeography of China* (Zhoa, 2009). For reproducibility, no other sources were referenced. Supplemental Table A (taxonomy) and Table B (chronology) lists our final 2104 genera, an increase of nearly 300 genera from a previous 2018 study.

Each genus was assigned to one of eight major taxonomic groups:

1) Agnatha. The thin-skinned jawless fish (Myllokunmingia, Pikaia, Haikouichthyes, hagfish), plus the conodonts.

2) Prostasianatha are defined as a polyphyletic group of jawless fish, agnatha, but with protective armor or scales. These include Pteraspidomorphi, Thelodonti, Heterostraci, Osteostraci, and Galeaspida.

3) Gnathostomata. Jawed fish, including Placodermi, plus the shark-like, Acanthodii, and Chondrichthyes.

4) Osteichthyes. Bony fish, including Actinopterygii (ray-finned fish).

5) Sarcopterygii (lobe-finned fish), but including the Dipnoi (lungfish), and Tetrapodomorpha (fish with "legs") such as Kenichthys and Tungsenia from China.

6) Basal Tetrapoda (lepospondyls, temnospondyls and reptiliomorpha).

7) Reptilia (Anapsida and Diapsida).

8) Synapsids (Pelycosaurs and pre-mammalian therapsids).

Geomagnetic activity during the Paleozoic shows two polarity superchrons (the Kiaman and Moyero) plus six polarity chrons lasting more than 6 million years. For simplicity we used a single source, Ogg's 2016 publication, to date polarity reversals and to delineate 17 Paleozoic zones. The nine zones with high levels of polarity reversals (HPZ) lasted for 124.9 million years (Ma). The eight zones with low-levels (LPZ) lasted 144.2 Ma. See Figure 1.

The Paleobiology database lists 37,800 occurrences of Paleozoic chordata genera (December 10, 2019). Each occurrence shows the geologic stage, "max_ma" and "min_ma" dates, plus taxonomy. From these occurrences, we determined the FAD (first appearance data) of 1665 genera. Spreadsheets from Benton and Sepkoski follow equivalent systematics. Zhoa and Zhu paper lacks a spreadsheet, but shows precise stratigraphy and chronology.

A genus is often dated entirely within the range of an LPZ or HPZ. But when the "max_ma" and "min_ma" are split by a dated polarity zone, we divided each genus proportionately. For example, the Lochkovian lasted from 419.2 to 410.8 Ma, but is split by a polarity zone at 416.5 Ma. Therefore, 32% of a Lochkovian genus is placed in the Upper Silurian HPZ10, and 68% in the Lower Devonian HPZ9. Proportionality is our only dating systematic. Refer to Supplemental Table C for the proportional dating of our 2104 genera.

PeerJ Preprints | https://doi.org/10.7287/peerj.preprints.28002v3 | CC BY 4.0 Open Access | rec: 31 Dec 2019, publ: 31 Dec 2019

Every genus is assigned to either early-phase (EP) or late-phase. The early phase—or early radiation—of our eight major clades has a start (FAD) and an endpoint. The endpoint could be placed exactly in-line with the FAD of a subsequent clade (zero overlap). Or the overlap could be a million years, or five million, or ten million years. The overlap might include all genera found in the same geologic stage, or in the same geomagnetic bin. Or we could view the Cambrian as the age of the conodonts; the Ordovician plus the Llandovery Stage as the age of the jawless fish; the Silurian as the age of the jawed fish; the Devonian as the age of the bony fish; the Mississippian plus the Bashkirian Stage as the age of the basal tetrapods; and the Pennsylvanian and Permian as the age of the reptiles and synapsids, and then use these "ages" to define the EP genera. For this study, each of these possibilities (overlaps, bins, or ages) will be used to calculate Pearson's coefficient.

Table 1: Distribution of early phase genera assigned to magnetic bins and placed in individual polarity zones.

Zones	Geologic stage	Early Chordata	Prostasiagnatha	Gnathastomata	Osteichthyes	Sarcopterygii	Basal tetrapoda	Reptilia .	Synapsida	Totals
HPZ-17	Late Permian								274	273.9
LPZ-16	Kiaman Superchron						11.2		95	106.6
HPZ-15	Westphalian A						32.2	0.9	0.9	34.0
LPZ-14	Pendleian Stage						12.1			12.1
HPZ-13	Late Visean						14			14.0
LPZ-12	Romer's Gap					2.4	12.3			14.7
HPZ-11	Late Devonian					49.5	15.2			64.7
LPZ-10	Middle Devonian			12.3		27.8				40.1
HPZ-9	Late Silurian			27.7	4	4.3				36.0
LPZ-8	Wenlock Stage		0.4	2						2.4
HPZ-7	Early Silurian		23.6	6						29.6
LPZ-6	Katian Stage		0.74							0.7
HPZ-5	Middle Ordovician		6.4							6.4
LPZ-4	Moyero Superchron		8.9							8.9
HPZ-3	Age 10, Late Cambrian	50								50.0
LPZ-2	Paiban Stage	5.7								5.7
HPZ-1	Early Cambrian	16.3								16.3

Table 1 shows the number of early-phase genera from our eight major vertebrate groups placed in individual geomagnetic polarity bins (reds are high-polarity zones; blues are low-polarity). The totals are used to calculate Pearson coefficient.

PeerJ Preprints | https://doi.org/10.7287/peerj.preprints.28002v3 | CC BY 4.0 Open Access | rec: 31 Dec 2019, publ: 31 Dec 2019

For this study, the first appearing genus of a major groups is critical.

1) The earliest known chordate is Hertzina, a conodont from the early Cambrian. HPZ-1.

2) The earliest Prostasianatha is placed by the scales of a jawless fish, Anatolepis (Upper Cambrian, middle Sunwaptan Stage, HPZ-3).

3) The earliest gnathostomes are the multiple acanthodian shark-fins found in China (Telychian Stage of the early Silurian, HPZ-7).

4) The earliest known Osteichthyes is the bony fish, Andreolepis, from the Ludlow Stage of the Upper Silurian, HPZ-9

5) The first member of our sarcopterygian group is the lungfish, Guiyu, also of the Ludlow Stage, HPZ-9.

6) The first basal tetrapods, as defined by Benton, is the lobe-finned fish, Livoniana, of the Late Givetian Stage in the Upper Devonian, HPZ-11.

7) The first reptile is Hylonomus of the Westphalian A Stage, HPZ-15, immediately prior to the Kiaman Superchron.

8) The first known synapsid, a pelycosaur, was also found in Westphalian A, HPZ-15.

Note that each of these originating genera were discovered in high-polarity geomagnetic zones.

Previous studies of the Cretaceous and Pleistocene have also shown a connection between geomagnetism and vertebrate evolution. Four mammal families initiated during the Cretaceous Normal superchron (.09 families per million years, Myr); eleven families in the period following the superchron (.63 families per Myr). The end-Cretaceous is when the first true placentals evolved (Halliday, 2019). The first continuous usage of stone tools began immediately after the Gauss-Matuyama geomagnetic polarity reversal (Semaw, 1997); the first all-purpose Acheulean hand axe was discovered in strata immediately above the Olduvai geomagnetic polarity chron (Lepre, 2011); the first solid evidence of continuous fire was found in a cave where multiple layers of carbon fibers and burnt bones occurred early within sediments of the short-term Jaramillo polarity chron (Berna, 2012); the Middle Stone Age Levallois core technique originated in approximate alignment with the CR-1 geomagnetic polarity collapse (Adler, 2014); displays of symbolism (ochre and beads) appear soon after the Blake geomagnetic polarity event (Hoffmann, 2018); figurative art and music (Floss, 2018), plus the demise of Neanderthals (Channell, 2019) started within a few hundred years of the Laschamp polarity collapse, 42 thousand years ago.

For this report, our preference is to analyze clades that phylogenetically led to hominins. Other paleontologists might not concur. Therefore, we ran statistical analyses both with and without reptilia.

PeerJ Preprints | https://doi.org/10.7287/peerj.preprints.28002v3 | CC BY 4.0 Open Access | rec: 31 Dec 2019, publ: 31 Dec 2019

Table 2 | Distribution of Paleozoic vertebrates within polarity zones.

Polarity Zones		Duration		Reversals		Distribution of Genera		
Zone	Geologic stages	Ma	Ma	GPRs	per Ma	EP genera	Total	%
HPZ-17	Late Permian	267.2-251.9	15.3	19	**1.24**	273.9	459.5	**59.6**
LPZ-16	Kiaman Superchron	315.1-267.2	47.9	10	**0.21**	106.6	522.3	**20.4**
HPZ-15	Westphalian A	319.3-315.1	4.2	9	**2.14**	34.0	50.2	**67.6**
LPZ-14	Pendleian Stage	330.2-319.3	10.9	6	**0.55**	12.1	54.7	**22.1**
HPZ-13	Late Visean	337.5-330.2	7.3	18	**2.47**	14.0	25.9	**54.2**
LPZ-12	Romer's Gap	356.5-337.5	19	6	**0.32**	14.7	89.2	**16.5**
HPZ-11	Late Devonian	388.6-356.5	32.1	42	**1.32**	64.7	256.8	**25.2**
LPZ-10	Middle Devonian	416.5-388.6	27.9	5	**0.18**	40.1	246.1	**16.3**
HPZ-9	Late Silurian	427.4-416.5	10.9	19	**1.78**	36.0	105.4	**34.2**
LPZ-8	Wenlock Stage	433.4-427.4	6	0	**0.00**	2.4	25.8	**9.2**
HPZ-7	Early Silurian	443.8-433.4	10.4	21	**2.00**	29.6	52.3	**56.7**
LPZ-6	Katian Stage	450.7-443.8	6.9	0	**0.14**	0.7	19.2	**3.9**
HPZ-5	Middle Ordovician	460.7-450.7	10	21	**2.10**	6.4	31.5	**20.2**
LPZ-4	Moyero Superchron	480-460.7	19.3	0	**0.00**	17.0	87.6	**19.5**
HPZ-3	Age 10, Late Cambrian	490.2-480	10.2	14	**1.37**	50.0	77.6	**69.7**
LPZ-2	Paiban Stage	496.5-490.2	6.3	0	**0.00**	5.7	22.9	**26.2**
HPZ-1	Early Cambrian	521-496.5	24.5	85	**3.47**	16.0	16.4	**100.0**

Table 2 shows the 17 high (red) and low polarity zones (blue), their range and duration (Ma), number of polarity reversals, reversals per million years, total genera in each polarity zone, early-phase genera, and their percentage found in each polarity zone. The Reversals per million years and percentage of genera are used to calculate Pearson's correlation coefficient.

Graphical Representation of Table C:

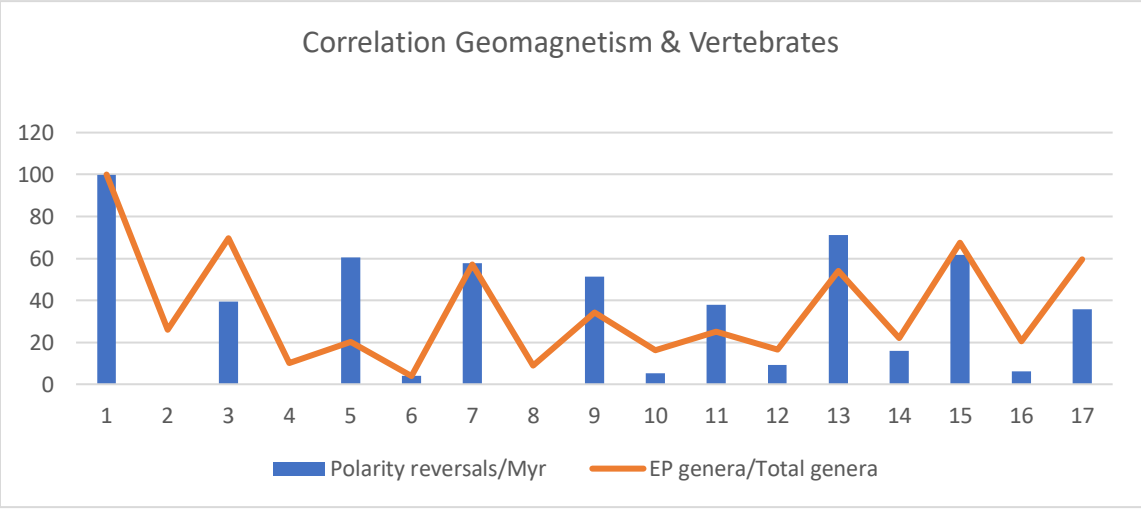

PeerJ Preprints | https://doi.org/10.7287/peerj.preprints.28002v3 | CC BY 4.0 Open Access | rec: 31 Dec 2019, publ: 31 Dec 2019

Results

Using the Paleobiology Database and Benton, Sepkoski, and Zhao, we compiled an Excel spreadsheet (see our supplemental tables) with 2104 Paleozoic genera. By chance, virtually half (1052.7 of 2104) of the total genera originated in a high-polarity zone. But of the 729.9 "early-phase" genera, 529.7 (72.5%) were found in high-polarity zones. Mutation rates equal 4.24 early-phase genera per million years in high-polarity zones, and 1.39 early-phase genera per million years in low-polarity zones. Marine genera were 195.5 of 261.7 (74.7%); terrestrial genera were 337.1 of 468.1 (72%).

Extrinsic biases such as outcrop area and accessibility are known to affect the distribution of fossils (Peters, 2001). Sample-size is a potential problem (for example, there are only four early-phase Osteichthyes compared to over 200 therapsids). To normalize these biases, we divided the early-phase genera by the total genera within each polarity zone, and then correlated those percentages to the rate of polarity reversals per million years for each of our high and low polarity zones to calculate Pearson's correlation coefficients (note the columns, "Reversals per Ma", and "percentages", in Table 2).

Pearson's correlation coefficients are calculated using Excel's statistical formulas:

1) Using geomagnetic bins, where all EP genera within the bin are counted, Pearson's correlation equals 0.819. Include all reptiles and Pearson's equals 0.776.

2) Cut off EP genera exactly at the first appearance of subsequent major group species (no overlap) and Pearson's correlation equals 0.7431.

3) Adding one million years to the first appearance of a subsequent major group species, and Pearson's equals 0.7430.

4) Add five million years, Pearson's equals 0.774.

5) But add ten million years, and Pearson's drops to 0.661, primarily due to the extension of the jawless fish later into the Silurian.

6) Count all pertinent species within a geologic stage and Pearson's equals 0.77.

7) Using geologic "ages" to determine EP genera, Pearson's equals 0.8185.

With geomagnetic bins, Social Science Statistics calculates Pearson's correlation coefficient at 0.8089, with a P-value of < .000084, by definition, a strong positive correlation.

Discussion

Although the statistical evidence shows a strong connection exists between the fossil record of Paleozoic vertebrates and polarity reversals, it does not determine if the causation is extrinsic (geologic) or intrinsic (biologic).

Fossilization is dependent on positive environmental conditions such as rapid burial or anoxia, and poor environmental conditions can cause gaps in the fossil record. Romer's Gap (LPZ-12) of the Early Carboniferous is now thought to be a sampling artifact (Anderson, 2015; Clack, 2016), but other gaps exist. The Middle Carboniferous Namurian Stage (LPZ-14) has

PeerJ Preprints | https://doi.org/10.7287/peerj.preprints.28002v3 | CC BY 4.0 Open Access | rec: 31 Dec 2019, publ: 31 Dec 2019

been called a gap in the tetrapod record (Clack, 2012). Olsen's gap runs between the last occurrence of pelycosaurs in North America until the earliest appearance of therapsids in the uppermost Kiaman superchron (LPZ-16). The Moyero Superchron (LPZ-4), shows active diversification of conodonts but limited occurrences of agnatha. The Cambrian Paibian (LPZ-2) gap lists only a single conodont, while the Upper Ordovician LPZ-6 is void of vertebrates other than conodonts. That these gaps correlate with low-polarity zones implies the causation is environmental, not biologic.

Volcanic activity, climate change, and the depletion of ozone have been linked to geomagnetic polarity reversals. But if these external causations are the connection, then why are invertebrates essentially unaffected? And after an indeterminant period of time, how do vertebrate families become immune to the ongoing effects of polarity reversals? Are DNA repair mechanisms involved?

Conclusions

In reality, evolution is a continuum with natural groups and clades merely artificial tools useful for clarification. Nonetheless, this continuum does not keep mutation rates from increasing periodically, nor does it keep the pace of evolution from accelerating during geomagnetic polarity collapses.

Detailed Methodology

Originally, we compiled a list of over 2000 Paleozoic vertebrate genera taken from multiple sources, but this early compilation lacked repeatability. Therefore, we limited our sources to the Paleobiology Database (downloaded December 10, 2019 from paleobioDB.org), Sepkoski's 2002 marine compilation, Benton's 2013 compilation, plus Zhao and Zhu's 2010 report. A single source would be ideal, but the Paleobiology Database still lacks many marine and terrestrial vertebrates, and their Phylum/Class/Order/Family taxonomy is often inadequate. Fossilworks (paleoDB.org) was referenced when needed to clarify taxon classification.

Any genus not listed in the four main sources was ignored. When dating with duplicate genera, Sepkoski had the lowest priority. Zhao and Zhu, with precise dating, had the highest. Otherwise, we chose the earliest, most precise date. For example, the paleobiology database does not divide the Visean into sub-stages, therefore, we used Benton's dating. We removed synonyms and uncertain genera. Imprecise dating >20 Ma was ignored, unless those dates were placed entirely within a single LPZ or HPZ.

Paleobiology's "max_ma" and "min_ma" dates were entered directly into our spreadsheet (in our previous report we used Gradstein and Ogg for dating purposes).

Dolichopareias, an early amphibian, is not Tournaisian. It is Upper Visean (the fossil, dated Visean, was discovered in 1927—a book written soon after made the dating error—see

PeerJ Preprints | https://doi.org/10.7287/peerj.preprints.28002v3 | CC BY 4.0 Open Access | rec: 31 Dec 2019, publ: 31 Dec 2019

paleobioDB). Recently, Xiushuiaspis, Changxingaspis, Meishanaspis, Sinogaleaspis, and Geraspis (galeaspids) were erroneously placed by PaleobioDB into the Sheinwoodian Stage using data from Zhu and Wang from 2000. But note, either Zhoa and Zhu's 2010 or 2018 report puts these fossils in the Telychian. Pentlandia, a dipnoid, is likely Devonian, not Lower Silurian. Pentlandia was removed from our datasheet.

The Cambrian presents a unique problem. There are 16 genera in the Early Cambrian HPZ-1, followed by 5.67 genera in LPZ-2 (See Table 2). When we divide the 5.67 genera by itself, the results unreasonably equal 100%. To compensate, we divide the 5.67 genera by the totals (16+5.67) to get 26.2%. Likewise, the 50 HPZ-3 conodonts calculated at 69.7% (50 divided by 16+5.67+50).

In addition, Cambrian chronology is unreliable. Of the 44 Cambrian Chordata only 32 have any precise. 13 are Early Cambrian (HPZ-1); 1 is Paibian (LPZ-2); with 18 in the Late Cambrian (HPZ-3).

The following Individual Paleozoic polarity reversals were taken entirely from Ogg's *A Concise Geologic Time Scale: 2016* (reds are high polarity zones; blues are low polarity zones). We extended the high-polarity zones by .2 myr after the uppermost polarity reversal in a zone (excluding the Silurian). Ogg's hatched magnetic zones are two reversals per million years. Note that all reversal times are approximate.

HPZ-17 (Guadalupian to Lopingian, Upper Permian): 252.1, 252.2-252.4, 252.8-253.2, 253.3-253.7, 253.8-255.9, 257.9-258.1, 260.1-260.8, 260.9-261.7, 268-268.1, 266-267.2.
LPZ-16 (Kiaman Superchron, Upper Carboniferous to Lower Permian): 286.3, 296.8, 299.1, 299.3, 300.5, 301, 304.8, 308.7, 311, 312.8 (each hatched zone counts as a single reversal)
HPZ-15 (Upper Bashkirian): 315.3-315.8, 316.1, 316.4, 316.8, 317-317.1, 318-319.3.
LPZ-14 (Upper Serpukhovian to Lower Bashkirian): 322.3, 323, 323.6, 324.1, 328.2-328.5.
HPZ-13 (Middle Viséan to Lower Serpukhovian, Carboniferous): 330.4-331.3, 331.8-331.9, 332.2-332.3, 333.1-333.3, 333.9-334.1, 334.7-334.9, 335.2-335.7, 336.5-336.8, 337.3-337.5.
LPZ-12 (Romer's Gap, Early Tournaisian to Middle Viséan, Carboniferous): 343, 343.6, 344.3, 346.0, 347.4, 352.3.
HPZ-11 (Givetian to Famennian, Upper Devonian, plus Early Tournaisian): 356.7-356.8, 357.5-357.7, 358.4-358.7, 359.5-359.6, ((363.6-365.2=1.6 Ma @2 rev/Ma=3.2 rev)), 366.7-370.1, 367.7-370.7, 371.6-372.8, 373.2-374, 374.8-376, 377.4-378.4, 378.7-378.9, 379.2, ((388.6-380.4=8.2 Ma @2 rev/Ma=16.4 rev)).
LPZ-10 (Middle Lochkovian to Eifelian, Lower Devonian): 393.3, 400.2-400.6, 401.7-402.
HPZ-9 (Ludlow to Pridoli Stages= 8.2 Ma at 2 reversals per million years = 16.4 plus Lower Lochkovian with 3 reversals to 416.7.
HPZ-8 (Wenlock Stage, Middle Silurian): none.
HPZ-7 (Llandovery, Lower Silurian): 10.4 Ma, at 2 reversals per million years = 20.8 reversals.
LPZ-6 (Middle Katian to Hirnantian, Ordovician): 448.7

PeerJ Preprints | https://doi.org/10.7287/peerj.preprints.28002v3 | CC BY 4.0 Open Access | rec: 31 Dec 2019, publ: 31 Dec 2019

HPZ-5 (Darriwilian to Lower Katian): 450.8-452.2, 452.4-452.9 453.7-454.2, 455.3-456.1, (((456.2,456.7, 457.2))) 457.7-457.9, 458.8-459.2, 459.4-459.5, 459.9-460.3, 460.6-460.7
LPZ-4 (Moyero Superchron, Upper Tremadocian to Lower Darriwilian):
HPZ-3 (Cambrian Age 10 to Lower Tremadocian): 482.1-482.5, 482.7-485.3, 485.6-486.4, 486.65-487.4, 486.85-486.9, 487.6-487.7, 490.15-490.2.
LPZ-2 (Paibian to Upper Jiangshanian): none
HPZ-1 (Lower Cambrian): 496.7-497.9, 497.45-497.5, 497.65-497.7, 497.85-497.9, 498-498.1, 498.3, 498.4, 498.8-498.9, 499.0-499.1, 499.5-499.6, 499.7-499.75, 499.8- 499.9, 500.1-500.2, 500.7-500.75, 500.8-501, 501.15-501.2, 501.4-501.6, 501.8-502, 502.2-502.3, 502.8- 502.9, 503.6-503.7, 504.1-504.8, 505.3-505.5, 506.7-507.2, 508.85-508.9, 509.2-509.5, 509.7-510.5, 510.65-510.7, 510.9-511.1, 512-512.1, (((512.4, 512.9, 513.4, 513.9, 514.4))) 515.8-515.85, 516.2-516.7, 516.6-516.9, 517.1-517.2, 517.5-517.6, 517.75-517.85, 518.1-518.2, 518.5-518.6, 518.8-519.3, 519.5-519.6, 519.8-520.

References

Adler, D.S. et al. (2014) Early Levallois technology and the Lower to Middle Paleolithic transition in the Southern Caucasus *Science* 345; 1609-13.

Anderson, J.S., Smithson, T., Mansky C.F. & Clack, J. A. (2015) Diverse Tetrapod Fauna at the Base of Romer's Gap. *PLoS One.*

Benton M.J., Ruta M, Dunhill A.M., Sakamoto M. (2013) The first half of tetrapod evolution, sampling proxies, and fossil record quality. *Palaeogeography, Palaeoclimatology, Palaeoecology* Vol. 372, 18-41.

Benton, M.J. (2015) *Vertebrate Palaeontology*, Fourth Edition. Wiley.

Berna, F. et al. (2012) Microstratigraphic evidence of in situ fire in the Acheulean strata of Wonderwerk Cave,Northern Cape province, South Africa *PNAS.*

Clack, J.E., et al. (2016) Phylogenetic and environmental context of a Tournaisian tetrapod fauna. *Nature Ecol & Evol.*

Clack, J.A. (2012) *Gaining Ground, The Origin and Evolution of Tetrapods* Indiana University Press.

Coates, M.J, Ruta, M. Freidman, M. (2008) Ever Since Owen: Changing Perspectives on the Early Evolution of Tetrapods. *Annu. Rev. Evol. Sys.* 39, 571-592.

Courtillow, V., Olson, P. (2007) Mantle plumes link magnetic superchrons to phanerozoic mass depletion events. *Earth and Planetary Science Letters* 260, 495-504.

Crutzen, P.J., Isaksen I.S., Reid, G.C. (1975) Solar proton events: Stratospheric sources of nitric oxide. *Science* 189, 457–459.

Floss,H. (2018) Same as it ever was? The Aurignacian of the Swabian Jura and the origins of palaeolithic art. *Quat Internat Vol 491.*

Glassmeier, K.H., Vogt J. (2010) Magnetic Polarity Transition and Biospheric effect, Historical Perspective and Current Developments. *Space Sci Rev* 155, 387-400.

PeerJ Preprints | https://doi.org/10.7287/peerj.preprints.28002v3 | CC BY 4.0 Open Access | rec: 31 Dec 2019, publ: 31 Dec 2019

Gradstein F.M., Ogg, J.G., Schmitz, M.D., Ogg, G.M. (2012) *The Geologic Time Scale* Elsevier.

Halliday, T.J.D. et al. Rapi morphological evolution in placental mammals post-dates the origin of the crown group Proceedings of the Royal Society B Vol 286, Issue 1898 (2019).

Harrison, C.G.A., Prospero, J.M. (1974) Reversals of the Earth's magnetic field and climate changes. *Nature* 250, 563-65.

Higham,T., et al. (2012) Testing models for the beginnings of the Aurignacian and the advent of figurative art and music: The radiocarbon chronology of GeiBenklosterle. *J. of Hum Evol*, Vol 62.

Hoffmann, D.L. (2018) Symbolic use of marine shells and mineral pigments by Iberian Neanderthals 115,000 years ago. *Science Advances* 4.

Huang, C. et al. (2017) The Contribution of Geomagnetic Activity to Polar Ozone Changes in the Upper Atmosphere *Advances in Meteorology* Volume 2017.

Kemp, T.S. (2005) *The Origin and Evolution of Mammals*.

Kemp, T.S. (2009) *Phylogenetic interrelationships and pattern of evolution of the therapsids: testing for polytomy.*

Kemp, T.S. (2012) The Origin and Radiation of Therapsids, in *Forerunners of Mammals* Chapter 1, edited by Chinsamy-Turan.

Kryza, R, et al. (2011) A SIMS zircon age for a biostratigraphically dated Upper Viséan (Asbian) bentonite in the Central-European Variscides (Bardo Unit, Polish Sudetes). *International Journal of Earth Science* Vol 11, Issue 6, pp 1227-1235.

Laurin, M. (2004) The Evolution of Body Size, Cope's Rule and the Origin of Amniotes. *Syst. Biol*. 53, 594-622.

Lepre, C.J., *et al*. (2011) An earlier origin for the Acheulian. *Nature* **477**.

Liboff, A.R. (2013) Weak-field ELF magnetic interactions: Implications for biological change during paleomagnetic reversals. *Electromagn. Biol. Med.* Volume 32.

McHargue, L.R. *et al*. (2000) Geomagnetic modulation of the late Pleistocene cosmic-ray flux as determined by ^{10}Be from Blake Outer Ridge marine sediments. *Nucl. Instrum. Methods Phys. Res. B* 172, 555–561.

Ogg, J.G., Ogg G.M. (2016) *A Concise Geologic Time Scale* Elsevier.

Pechersky D.M., Lyubushin A.A., Sharonova Z.V. (2012) On the Coherence between Changes in Biota and Geomagnetic Reversals in the Phanerozoic. *Russian Academy of Sciences*, Vol. 48 44-62.

Peters, S.E. and Foote, M. (2001) Biodiversity in the Phanerozoic: a reinterpretation. *Paleobiology* 27, 583-601.

Raisbeck, G. M., Yiou, F., Cattani, O., Jouzel, J. (2006) ^{10}Be evidence for the Matuyama–Brunhes geomagnetic reversal in the EPICA Dome C ice core". *Nature* 444: 82–84.

Sansom R.S., Randle, E., Donoghue, P.C.J. (2014) Discriminating signal from noise in the fossil record of early vertebrates reveals cryptic evolutionary history. *Biol. Sci*. 282.

PeerJ Preprints | https://doi.org/10.7287/peerj.preprints.28002v3 | CC BY 4.0 Open Access | rec: 31 Dec 2019, publ: 31 Dec 2019

Sassi, M, et al. (2014) Carbon-14 decay as a source of non-canonical bases in DNA. *Biochimica et Biohysica Acta*.

Sepkoski, J.J. (2002) A compendium of fossil marine animal genera. *Bulletins of American paleontology*. No. 363.

Semaw, S.(1997) 2.6-Million-year-old stone tools and associated bones from the OGS-6 and OGS-7, Gona, Afar, Ethiopia. *Journal of Human Evolution* 45, 169-177,

Smith, M.P., (2007) The Cambrian origin of vertebrates, in *Major Events in Early Vertebrate Evolution, Palaeontology, phylogeny, genetics and development*. Edited by Per Erik Ahlberg..

Staub, J.P. (2018) Paleozoic geomagnetism shapes vertebrate evolution. *PeerJ*

Uffen R.J., (1963) Influence of the Earth's core on the origin and evolution of life. *Nature* 198, 143–144.

VanHuizen et al. (2019) Weak magnetic fields alter stem cell-mediated growth. *Science Advances*.

Wei, Y. *et al*. (2014) Oxygen escape from the Earth during geomagnetic reversals: Implications to mass extinction. *Earth and Planetary Science Letters* 394, 94-98.

Xi-Ping, Bergstrom Middle and Upper Cambrian Protoconodonts and Paraconodonts from Hunan, South China.

Zhao, W.J., Zhu, M. (2010) Siluro-Devonian vertebrate biostratigraphy and biogeography of China. Palaeoworld 19, 4-26.

Zhu, M. *et al*. (2009) The oldest articulated osteichthyan reveals mosaic gnathostome characters. *Nature* 458, 469-474.

PeerJ Preprints | https://doi.org/10.7287/peerj.preprints.28002v3 | CC BY 4.0 Open Access | rec: 31 Dec 2019, publ: 31 Dec 2019